RESEARCH ARTICLE

Broad Scaling Region in a Spatial Ecological System

MANOJIT ROY,[1] MERCEDES PASCUAL,[1] AND ALAIN FRANC[2]

[1]*Department of Ecology and Evolutionary Biology, University of Michigan, Ann Arbor, Michigan 48109-1048*

[2]*INRA, Forest and Natural Environment Department, Paris, and Orsay University, Laboratory ESE, France*

Received August 16, 2002; revised March 11, 2003; accepted June 3, 2003

The ubiquity of scale-free patterns in ecological systems has raised the possibility that these systems operate near criticality. Critical phenomena (CP) require the tuning of parameters and typically exhibit a narrow scaling region in which power laws hold. Here we show that an individual-based predator-prey model exhibits scaling properties similar to CP, generated by a percolation-like transition but with a broader scaling region. There are no drastic changes in ecological quantities across this critical point and species coexist broadly in parameter space. The implications of these findings for the stability of ecological systems "near" criticality is discussed. © 2003 Wiley Periodicals, Inc.

Key Words: criticality; robust power-law scalings; self-organization; percolation; individual-based predator-prey model

1. INTRODUCTION

The search for explanations of scale-free patterns in nature, and the ubiquitous power laws that characterize them, has raised the possibility that ecological systems operate near criticality [1–4]. Explanations related to criticality are of interest because they have implications for the sensitivity of systems to external perturbations and for the occurrence of large and unpredictable intermittent fluctuations [5–8].

Corresponding author: Mercedes Pascual, E-mail: pascual@umich.edu

"Critical phenomena" (CP) provide a well-known mechanism for generating power laws in systems with a large number of interacting components at equilibrium [9]. Typically, CP are accompanied by a phase transition, in which the global state of the system undergoes a drastic change when one or more parameters are *tuned* to a specific value, known as the "critical point" [10]. For example, the spatial spread of disease modeled as a contact process exhibits a breakpoint at which the infected state becomes established [2]. A number of power laws hold at or near the critical point, which are used to characterize CP. These power laws include the well-known relationship between a control parameter, which can be externally controlled (tuned), and an order parameter, which is a variable reflecting the change in

the state of the system across the critical point. The tuning of CP, and the associated extreme sensitivity to changes in parameter values, are difficult to account for in ecological systems that are typically subject to frequent environmental fluctuations. An alternative mechanism capable of generating power laws has been proposed in the phenomenon of "self-organized criticality" (SOC) [11,12]. SOC, as the name suggests, provides a self-organizing mechanism for generating power law scalings in an open system that is slowly driven [12]. These scalings are robust to perturbations because the system takes itself to the critical state regardless of parameter values. The temporal dynamics of the system display, however, variations of all sizes including large and unpredictable intermittent fluctuations [2,6,13]. For systems so far found to exhibit SOC, the question of whether they really differ from classical CP is a subject of current debate [9,14], with efforts to map the former onto the latter in particular cases [15,16]. The contention lies in the argument that the slow driving needed by SOC may provide the external tuning for CP.

In this article, we propose another possible explanation for robust power laws that hold broadly in parameter space. With a spatial predator-prey model that is individual-based and stochastic, we show that this explanation involves a critical phase transition, but one at which there is no drastic change in the biological variables of interest. Thus, both populations persist broadly in parameter space and their abundance changes continuously across the critical point. This "hidden" transition is revealed, however, by a drastic change in the size of prey clusters and in the associated connectedness of the system. We specifically show that the origin of the power laws is a transition with similarities and differences to that of percolation. We focus in particular on the exponent that is relevant to the width of the critical region.

The implication of this type of behavior is that the scalings typical of criticality are possible without either the extreme sensitivity to perturbations typically associated with other examples of CP in ecology, or the large intermittent temporal fluctuations of SOC. These observations raise the possibility of a greater temporal stability than that typically associated with patterns of criticality. We discuss the relevance of these findings for other systems with antagonistic interactions, such as those for host-parasite and disturbance-recovery dynamics and for systems that are not necessarily closed. It may be noted here that there exist lattice-based predator-prey models that exhibit a sharp transition from uniform prey cover to a predator-prey coexistence under explicit tuning [17]. Such models belong to a class of CP known as "directed percolation," which also includes systems involving contact processes [9,14]. It is also well known that all power laws are not critical, with many alternative models to explain scalings [9]. They include mechanisms as diverse as the distribution of residual lifetimes, superposition of distributions, random walks, multiplicative noise with constraints, highly optimized tolerance etc. We are, however, interested here exclusively in mechanisms involving the collective behavior of a large number of interacting components as in CP and SOC, which is relevant to the local interaction of individuals in ecological systems.

Finally, our results have implications for the relationship between connectedness and sensitivity to perturbations in ecological systems. The adaptive cycle metaphor of Holling and colleagues [18] describes the temporal changes in the potential to accumulate resources, such as nutrients or biomass, of ecosystems as a function of connectedness. These changes are primarily viewed in a temporal context and explained through the coexistence of multiple steady states. When space is considered, the possible analogy to SOC has been discussed [18]. There is a need for a better understanding of the different ways in which connectedness and resilience are related in the dynamics of biological systems with distributed interactions. Key determinants of this relationship most likely regard the relative temporal scales of these interactions, in space or in other types of networks.

2. THE MODEL

Space in the model is implemented as a 2D lattice in which each site is either occupied by a prey, a predator, or is empty [19,20]. These three states allow us to incorporate the two basic processes of local antagonistic interactions, namely the spread of disturbance (by the predator) and the regrowth or recovery (by the prey). All processes are local with the range limited to its four nearest neighbor sites. Thus, the model is an extension of a boolean contact process [22,23] in which each site has three possible states.

A prey samples a neighboring site at random and if empty, gives birth onto it at a rate α_1. A predator hunts for prey by inspecting all of its neighbors at a rate 1. If preys are found, the predator chooses one at random, eats it, moves onto this site, and produces an offspring with probability α_2 which occupies the original site. If preys are not found, the predator starves and dies with probability δ. There is dispersive movement through random mixing: neighboring sites exchange states at a constant rate. Thus, the model incorporates demographic stochasticity: events such as birth, death, and movement are all Poisson processes with associated probabilistic rates. All simulations are run with periodic boundary conditions.

Simulations have shown that the system converges to a stationary state in which predator and prey coexist for a broad range of parameters: $0 < \alpha_1, \alpha_2, \delta < 1$. It approaches the two "absorbing" states of uniform prey cover ($p = 1$, $h = 0$) and total extinction (p, $h = 0$) at the extreme parameter values $\alpha_2 = 0$, $\delta > 0$ and $\alpha_2 \approx 1$, $\delta \approx 0$, respectively [21]. There are three global stationary states: an "active state" of coexistence of all three local states ($0 < p + h < 1$), and the

FIGURE 1

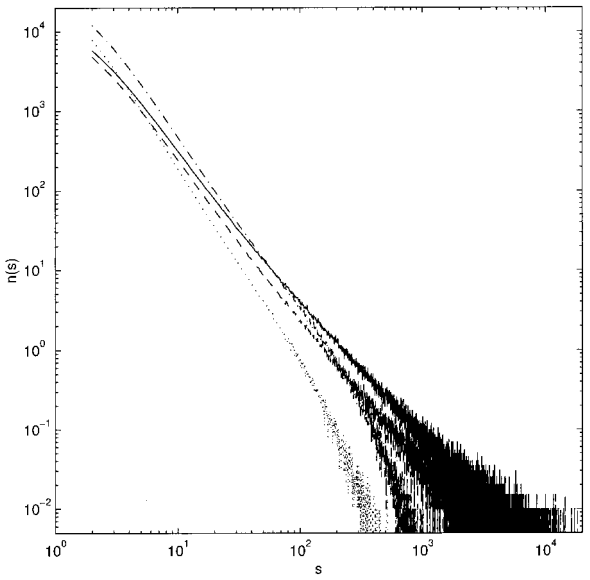

Prey cluster distribution $n(s)$ versus s on a log-log scale, for four values of $\varepsilon = \alpha_2/(\alpha_2 + \delta)$, 0.082, 0.1, 0.4 and 0.7 (continuous, dashed, dashed-dotted, and dotted lines, respectively). Least-square estimates of the respective slopes give the scaling exponents $\gamma =$ 1.81, 1.93, 2.14, and 2.39. ($L = 1000$ and $\alpha_1 = 0.5$).

two absorbing states mentioned above. In the coexistence regime a number of power laws have been previously described for the spatial distribution of the prey [21,25]. In particular, the size distribution of prey clusters exhibits a power law decay for a broad range of parameter values (Figure 1). The range of this scaling decreases for parameters leading to low density of the prey, as expected for clusters that achieve smaller maximum sizes. We return to these patterns later.

To investigate the origin of these patterns, we demonstrate in the following sections that the system exhibits two continuous phase transitions: one between the active state of coexistence and the absorbing state of uniform prey cover; the other, a percolation-like transition, well within the domain of the active state. The former transition is biologically trivial in the sense that full occupancy of space by the prey, and the corresponding extinction of the predator, are expected at the lowest possible growth and/or high mortality of the predator. Nevertheless, its existence allows us to establish a critical relationship between a control and an order parameter in the system. The rest of the article focuses on the second transition and on its consequences for the existence of robust scaling properties in the spatial distributions of individuals.

3. ACTIVE-ABSORBING STATE TRANSITION

The first transition we address is an "active-absorbing transition" (AAT) in which the system goes from the active state of prey-predator coexistence ($0 < p, h < 1$) to the absorbing state of full space occupancy by the prey ($p = 1$, $h = 0$). It is possible to map this transition to the critical point of an order-control parameter relationship, by suitably defining an order parameter m and a control parameter ε. The order parameter m is typically defined such that $m = 0$ for the control parameter on one side of the critical point ε_{c1}, and $m > 0$ on the other side of this point. The order-control relationship for a continuous phase transition is then described by a power law

$$m \propto (\varepsilon - \varepsilon_{c1})^{\beta}, \tag{1}$$

with an exponent β, which holds only when ε is "tuned" very close to ε_{c1} [10].

To identify the control parameter ε for our system, we introduce the probability π of isolation of a predator, defined as the probability that a randomly chosen predator has no prey in its neighborhood. It has been shown that π satisfies the relationship

$$\pi = (1 - p)^{q}, \tag{2}$$

where p is the prey density and the exponent q is the "modified" neighborhood size of a predator [24,25]. Under mean-field assumptions, when individuals are well-mixed and interact at mean densities, Eq. 2 holds trivially with $q = 4$, the original neighborhood size. The "modified" value of q corrects for the decrease in the predation rate at the aggregated population level due to the spatial heterogeneity in the distribution of individuals [25]. The mean-field birth and death of predators can be written as $\alpha_2 h(1 - \pi)$ and $\delta h\pi$, respectively. With these expressions, the dynamics of the predator's density h are given by the following equation,

$$\frac{dh}{dt} = \alpha_2 h(1 - \pi) - \delta h\pi. \tag{3}$$

Thus, at stationarity ($dh/dt = 0$), the probability of isolation of the predator also satisfies

$$\pi = \frac{\alpha_2}{\alpha_2 + \delta}. \tag{4}$$

This expression allows us to rewrite here Eq. 2 in the form

$$m = (\varepsilon - \varepsilon_{c1})^{\beta}, \quad \varepsilon = \frac{\alpha_2}{\alpha_2 + \delta}, \tag{5}$$

FIGURE 2

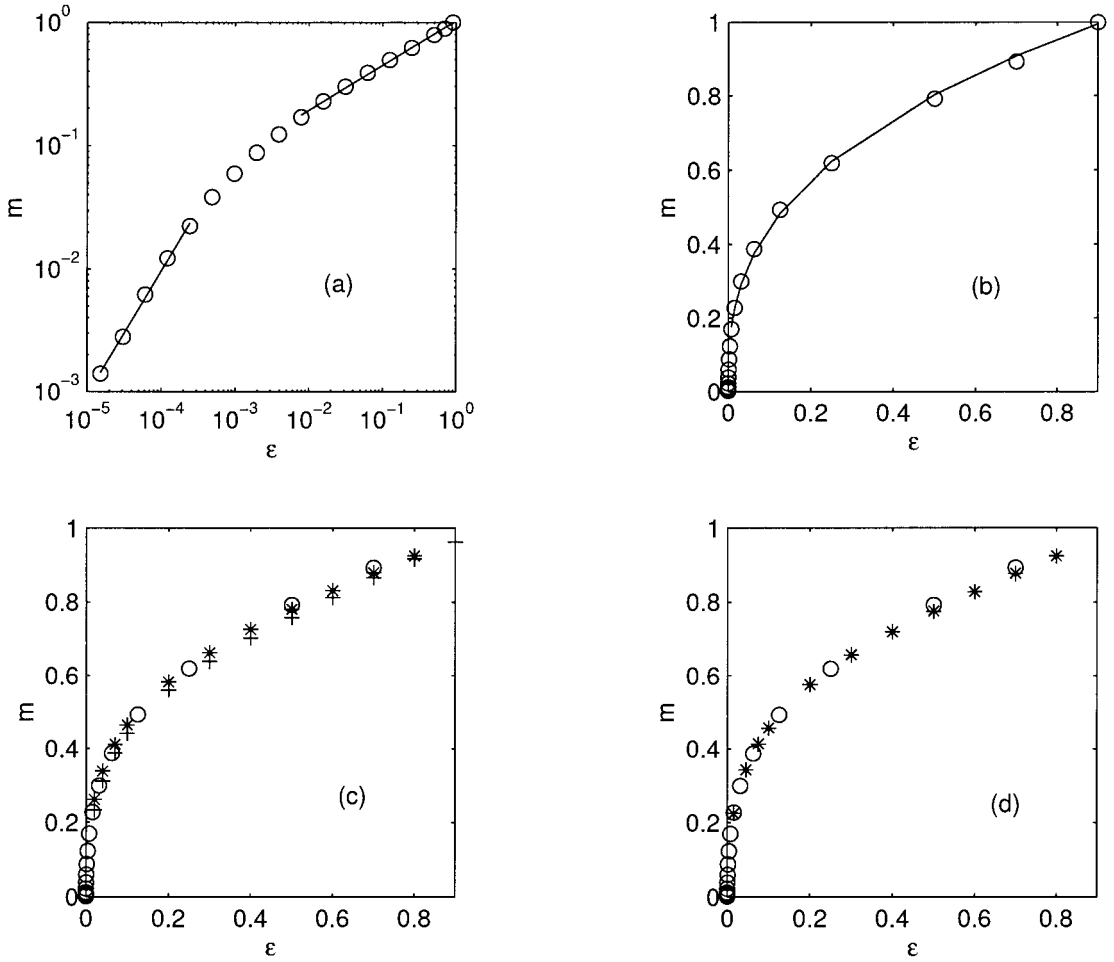

(a) Order parameter $m = 1 - p$ as a function of the control parameter ε on a log-log scale. The open circles are obtained by simulating the model in a grid of size $L = 500$ and with $\alpha_1 = 0.5$. The points are averages over 1000 snapshots, each 20 timesteps apart (after transients are discarded). The straight line segments in the two intervals $\varepsilon \leq 0.0002$ and ≥ 0.01 correspond to least-square fits of Eq. 5, with respective slope estimates $\beta = 1.013$ and 0.365. (b) The same curve is shown with a linear scale. The continuous line corresponds to the fit with $\beta = 0.365$. (c) m-ε plots for three α_1 values equal to 0.2, 0.5, and 0.8 (+, ○, and ∗, respectively). (d) m-ε plots for three grid sizes $L = 50$, 200 and 500 (+, ×, and ○, respectively; $\alpha_1 = 0.5$).

with $m = 1 - p$, $\varepsilon_{c1} = 0$, and $\beta = 1/q$. Equation 5 provides a critical scaling relation similar to Eq. 1 with $1 - p$ as the order parameter and $\alpha_2/(\alpha_2 + \delta)$ as the control parameter. For the absorbing state, $m = 0$, which occurs for $\alpha_2 = 0$, $\delta > 0$, and therefore for $\varepsilon = 0 = \varepsilon_{c1}$. In the coexistence regime, $m > 0$, which holds for $0 < \alpha_2$, $\delta < 1$, that is for the whole range of possible nontrivial values of the growth and survival of the predator given by $\varepsilon_{c1} < \varepsilon < 1$.

The above argument gives an analytical basis for the existence of an active-absorbing state transition in the system at the point $\varepsilon_{c1} = 0$. Next we numerically verify Eq. 5 by estimating the equilibrium prey density p as ε is varied from 0 to 1 (by changing α_2 and δ) in a grid of size $L = 500$. Figure 2(a) shows m as a function of ε on a log-log scale, with the prey growth rate $\alpha_1 = 0.5$. Two distinct linear regimes are clearly visible for $\varepsilon \leq 0.0002$ and $\varepsilon \geq 0.01$. Least-square estimates of their respective slopes yield the exponents $\beta = 1.013$ and 0.365, respectively. The second estimate corresponds closely to the value of $q = 2.75$ previously obtained in numerical estimates of the modified neighborhood size [25]. This value was used to correct the mean-field predation rate to approximate the large scale dynamics of population densities [25]. Furthermore, this agreement holds for almost the whole range of possible values of ε, away from the trivial case of $\varepsilon \approx 0$. This agreement is clear from Figure 2(b), which replots m as a function of ε on a linear scale and compares it with the analytical expectation for $\beta(=1/2.75 = 0.364)$.

Figure 2(c) shows the m-ε curves for three different values of the prey's growth rate. The plots appear insensitive to changes in α_1 for almost the whole range of ε. Figure 2(d) shows the same curves for three different grid sizes L = 50,200, and 500 and for the original value of $\alpha_1 = 0.5$. The curves exhibit remarkable agreement independent of system size [17]. The existence of this second scaling region away from zero and within the domain of coexistence motivates our search for a second critical point.

4. THE PERCOLATION-LIKE TRANSITION

We show next that the system exhibits a percolation-like transition (PLT) associated with a second critical point ε_{c2} within the domain of predator-prey coexistence. Unlike AAT, the presence of this point is not indicated by an obvious transition in the biological state of the system, because both prey and predator coexist on either side of PLT. However, a rapid build-up of spatial correlation for the prey occurs close to ε_{c2}, leading to the formation of a spanning prey cluster similar to that of percolation [26]. A "cluster" is defined as a group of similar sites (here prey sites) connected by at least one of the four nearest neighbors, and a "spanning cluster" refers to one that spans the grid end-to-end.

Figure 3 shows the location of the critical point ε_{c2} across which the spanning prey cluster appears in a grid of size L = 1000. P_∞ is plotted as a function of the control parameter ε, where P_∞ is given by the fraction of 200 snapshots that contain at least one spanning prey cluster [Figure 3(a)]. This curve approximates a step function of the type

$$P_\infty(\varepsilon) = \begin{cases} 1 & \text{for } \varepsilon \le \varepsilon_{c2}, \\ 0 & \text{for } \varepsilon > \varepsilon_{c2} \end{cases}$$

as expected for a percolation-type transition. If we define the critical point ε_{c2} as the value of the control parameter for which $P_\infty(\varepsilon_{c2}) = 0.5$, we obtain $\varepsilon_{c2} = 0.082$. Furthermore, this value of ε corresponds to an equilibrium prey density $p_c = 0.575$ close to the percolation threshold density of 0.592 [26]. Figure 3(b) shows P_∞ as a function of p, which approximates again a step-function across p_c. We also plot s_∞, the size of the spanning prey cluster normalized by the size of the grid. By definition $s_\infty = 0$ for $p < p_c$ and $s_\infty > 0$ for $p \ge p_c$.

Having established a PLT in the system with an associated critical point ε_{c2} and corresponding p_c, we address next how this transition governs the various spatial patterns that the model exhibits. We concentrate on the right-hand side of this transition, away from the trivial extreme of low ε. As ε decreases below ε_{c2} (or equivalently p increases above p_c), s_∞ rises steadily and the spanning prey cluster, as expected, begins to fill up the entire grid. On the opposite side, the window $\varepsilon_{c2} \le \varepsilon \le 1$ comprises the bulk of the permissible range of ε values giving rise to coexistence. In this window, a rich variety of interesting patterns occur.

FIGURE 3

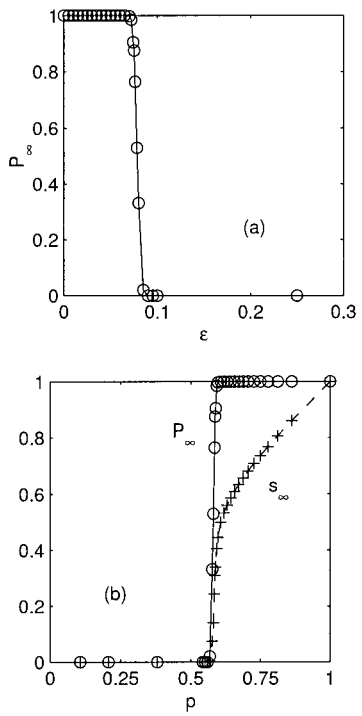

(a) P_∞ as a function of ε, obtained by averaging over 200 snapshots, each 20 timesteps apart, after discarding 20000 transients (L = 1000 and $\alpha_1 = 0.5$). (b) P_∞, s_∞ as a function of prey density p. The ε-scale is restricted to [0, 0.3] for better zooming of the region. (See text for definitions).

4.1. Correlation Length

The correlation structure of a system provides an important characterization of its spatial patterns. The *correlation function* or pair-connectivity $C(r)$ for the prey is defined as the probability that two prey sites a distance r apart from each other belong to the same prey cluster [26]. Contributions of only the finite clusters are considered in estimating this function (spanning clusters are excluded for $\varepsilon \le \varepsilon_{c2}$), so that $C(r)$ exhibits the expected decay pattern with increasing r on both sides of criticality. The correlation function $C(r)$ has the following general dependence on r,

$$C(r) \propto r^{-\delta} \exp\left(\frac{-r}{\xi}\right), \tag{6}$$

where ξ is the *correlation length,* defined as the average distance between two prey sites belonging to the same cluster [26]. At criticality (ε_{c2}), ξ diverges in an infinite sys-

FIGURE 4

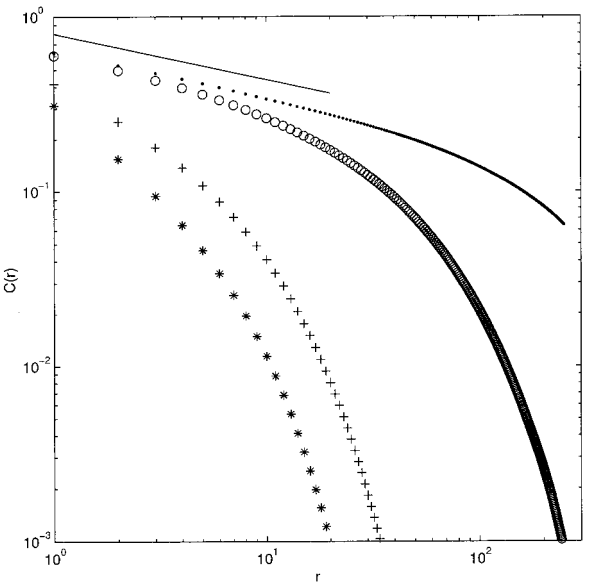

Log-log plots of the correlation function $C(r)$ as a function of distance r for prey sites, and for four values of $\varepsilon = 0.082$, 0.1, 0.4 and 0.7 (., ○, +, and ∗, respectively; $L = 500$ and $\alpha_1 = 0.5$). For comparison, the straight line at the top illustrates a slope $\delta = 0.263$ corresponding to the least-square fit for the critical value of $\varepsilon = 0.082$ (see text for details).

tem because of the appearance of large clusters of the order of the system size, and Eq. 6 reduces to a pure power law

$$C(r) \propto r^{-\delta}. \tag{7}$$

In finite systems, a finite-size cutoff is present. The correlation length ξ is finite and decreases in magnitude as ε moves away from ε_{c2} on either side, thereby making the exponential term in Eq. 6 dominate over the power law. Figure 4 illustrates these patterns for our model. $C(r)$ is plotted as a function of r on a log-log scale for $\varepsilon_{c2} = 0.082$, 0.1, 0.4 and 0.7. The plot at criticality shows a linear regime for $r \leq 30$, whose slope is $\delta = 0.263$. The scaling deteriorates progressively for higher ε, resulting in increasingly steeper exponential decays as predicted by Eq. 6. To examine the speed of the decay as we move away from the critical point, we consider next an exponent describing how correlation length varies with distance from this point.

The correlation length ξ for percolation exhibits the following relationship close to the critical point,

$$\xi \propto |p - p_c|^{-\nu}, \tag{8}$$

and a nonrigorous argument, supported by numerical estimates, gives $\nu = 4/3$ [26]. We compute ξ for our system using the formula [26]:

$$\xi^2 = \frac{\sum_r r^2 C(r)}{\sum_r C(r)},$$

and plot it against the equilibrium prey density p. Figure 5(a) shows these plots for four different grid sizes $L = 128$, 256, 512, and 1024. All curves exhibit a peak near the critical density $p_c = 0.575$, and the peak decreases with L as expected. If the differences are due only to finite-size effects, it should be possible to collapse all curves onto a single one by rescaling ξ as follows:

$$\xi(p, L) \rightarrow L^{-a}\xi(L^b(p - p_c)),$$

with finite-size scaling exponents a and b. As Figure 5(b) demonstrates, such a rescaling is indeed possible for $a = -1$ and $b = 1$.

A comparison with the results for percolation can help determine how fast or slow ξ diverges at criticality in our model relative to percolation. From Eqs. 8 and 6, it is easy to see that the exponent ν, which determines the rate of divergence of ξ at criticality, also determines the importance of the exponential term relative to the power law dependence for $C(r)$ away from criticality. The lower the value of ν, the wider the region $|p - p_c|$ and thus $|\varepsilon - \varepsilon_{c2}|$, over which ξ remains appreciably large. Thus, a lower ν value effectively "broadens" the region over which the $C(r)$ scaling holds. For the purpose of comparison, we estimate the $\xi - p$ values for random-site percolation with the same four grid sizes L and show the corresponding collapsed plots in Figure 5(c). They peak at $p = 0.592$ as expected, and the finite-size scaling exponents are $a = -1$ and $b = 0.9$. Clearly, the divergence for percolation is sharper than that for our system. We quantify this observation by estimating the exponent ν for both. Figure 5(d) shows, on a log-log scale, the rescaled ξ versus $|p - p_c|$ plots for the spatial predator-prey system and for percolation ($p < p_c$). The straight lines are least-square fits, with estimates $\nu = 0.93 \pm 0.02$ for the predator-prey model and $\nu = 1.20 \pm 0.003$ for percolation (which agrees reasonably well with 4/3). The significantly lower ν for our model implies a more robust correlation scaling away from criticality. We have also compared Figure 4 against percolation plots with similar density differences (not shown), confirming this observation. We return below to another scaling characterizing the spatial patterns in the system, that of the cluster size distributions.

4.2. Prey Cluster Distribution

The cluster size distribution for percolation exhibits a power law decay at criticality of the form

$$n(s) \propto s^{-\gamma}, \tag{9}$$

where $n(s)$ denotes the number of clusters of a given size s, and the exponent $\gamma(=2.05)$ is known as the Fisher exponent

FIGURE 5

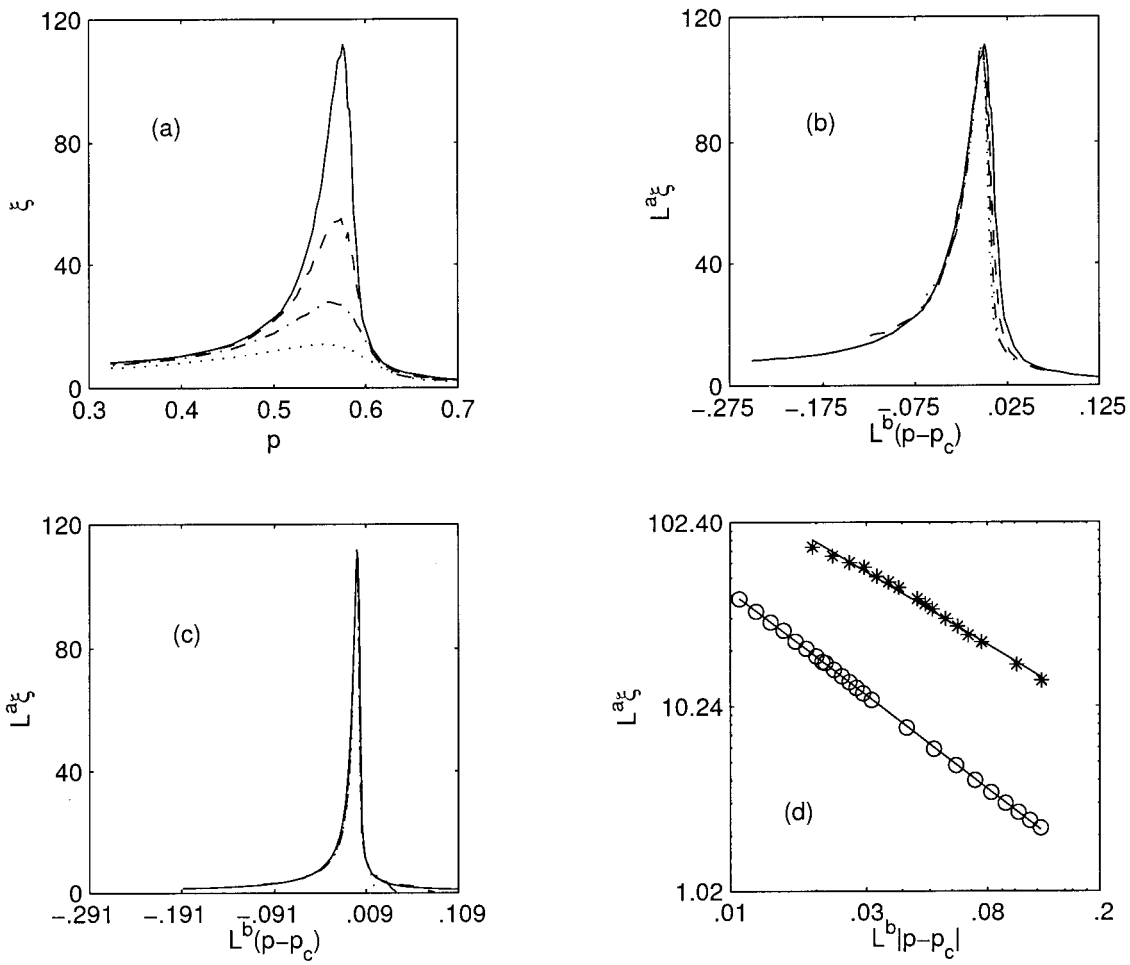

(a) Correlation length ξ as a function of equilibrium prey density p for grid sizes $L = 128$, 256, 512, and 1024 (dotted, dashed-dotted, dashed, and continuous lines, respectively; $\alpha_1 = 0.5$). (b) The same curves collapsed on rescaled axes [Axes' ranges in (c) and (b) are kept the same for comparison]. (c) Rescaled curves for site percolation using the same four grid sizes. (d) Rescaled $L = 1024$ plots for the model (∗) and percolation (○) on a log-log scale, for $p < p_c$. The straight lines are least-square fits, giving estimates for the exponent ν of 0.93 and 1.20, respectively (see text for details).

[26]. Away from criticality this scaling rapidly gives way to an exponential decay pattern similar to that of the correlation function $C(r)$.

We return here to Figure 1, which shows the prey cluster distribution in our model for different values of the control parameter ε. All four plots exhibit a linear regime indicative of a power law, with a scaling range that decreases for ε above ε_{c2}. This decrease is due to the fact that as ε increases, the density of prey p decreases, and prey clusters become fewer and smaller, giving rise to an exponential cutoff. (The respective ε values correspond to $p = 0.575(=p_c)$, 0.543, 0.280, and 0.122). Least-square estimates of the scaling exponents yield $\gamma = 1.81$, 1.93, 2.14, and 2.39, respectively, indicating a steeper decay as one moves away from criticality. The values remain, however, within a narrow range given the wide change in prey density (see also, [21]). A comparison with percolation using the same density differences confirms that the power-law scaling in our model holds for a much broader range of p (not shown). This pattern is consistent with the build-up of correlations from local interactions and the related wider critical region described in the previous section. These observations for correlation length and size distributions also hold for a wide range of reproductive rates of the prey α_1 (not shown).

5. CONCLUSIONS

In summary, our individual-based spatial predator-prey model exhibits a set of scaling properties characteristic of systems near criticality. A percolation-type transition, at which finite clusters of the prey give rise to a spanning

cluster, explains the origin of these power laws in the system. One significant difference with percolation is, however, the broader parameter region for which the scalings hold. This difference is consistent with a lower value of the scaling exponent relating the correlation length to the equilibrium density of the prey. It follows that critical phenomena of the type described here are a viable explanation for power laws in nature: scaling regions need not be confined to too small a region of parameter space. The patterns are reminiscent of the "broad phase transition" observed in the percolative spread of epidemics when susceptibility is random [28], and in the 2D XY spin system which is critical over the entire low temperature region [29,30]. Scaling behavior of the cluster size distribution in a narrow temperature range away from, but close to, the critical point has been described for simulations of the Ising model [31]. In three dimensions, these simulations have also shown the existence of a percolation-type transition below the critical point.

In our model there is no drastic change in population abundances at criticality and the species coexist on either side of this transition. Indeed, coexistence occurs for the whole range of possible values of the control parameter and is insensitive to the existence of this critical point. A drastic change occurs, instead, in the geometry of the system and in particular in its connectedness. These results underscore that the existence of power-law scalings need not imply the high sensitivity to external perturbations typically associated with CP. The critical point is, however, not far from another transition at which the predator does go extinct. Whether this proximity between the two critical points is generally the case remains to be determined.

As noted before, Self Organized Criticality requires a slow and sustained external driving that is not present in our predator-prey system. It may be argued that this property would limit the relevance of the predator-prey model since ecological systems are typically open. We conjecture, however, that the power-law phenomena reported here are not restricted to closed systems. Indeed we expect that similar scalings may apply to other spatio-temporal models with local antagonistic interactions, particularly those whose well-mixed counterparts exhibit decaying or sustained oscillations in time as in the predator-prey model. Previous studies already indicate that a spatial model for the local spread of disturbance and recovery in a mussel bed, which incorporates a steady input of external new disturbances, exhibits very similar spatial properties and a percolation-type transition [21,32]. Interestingly, the rate of this input is not necessarily slow compared to the intrinsic time scales of the system. Thus, both the disturbance-recovery and the predator-prey model lack the separation of time scales present in forest-fire and epidemic models that exhibit SOC [6,7,33,34]. This difference is closely related to the lack of large intermittent fluctuations in the temporal dynamics of the predator-prey system. Population densities of the predator and prey measured at the spatial scale of the whole grid exhibit small fluctuations around an apparent steady-state [24]. It remains to be determined whether quantities other than population densities, in particular those associated with the clusters in the system, display temporal characteristics similar to those of SOC.

Finally, the implications of connectedness for ecosystem stability, in the specific sense of resilience by Holling [18], need to be better understood. One definition refers to the magnitude of external perturbations that can be sustained before an important change occurs in the variables and processes that control behavior. As shown here, connectedness alone is not sufficient to understand resilience. The view of ecosystem dynamics as an adaptive cycle is based primarily on temporal considerations [18] (but see [35]). Limited analogies to SOC have been drawn in a spatial context [18]. Extensions of this view to the spatial dimension should consider the different types of critical systems that are now possible for the spatio-temporal dynamics of disturbance and recovery. Perhaps a better understanding will follow from a classification of systems with distributed interactions, based on the relative temporal scales of their underlying processes.

ACKNOWLEDGMENTS

We thank Henrik Jensen and Frederic Guichard for helpful comments. We also thank Jerome Chave for an insightful review of an earlier version of this manuscript that pointed us in the right direction. This work was supported by a Centennial Fellowship of the James S. McDonnell Foundation to M.P.

REFERENCES

1. Solé, R.; Manrubia, S. Are rainforests self-organized in a critical state? J Theor Biol 17, 1995, 31–40.
2. Solé, R.V.; Manrubia, S.C.; Kauffman, S.; Benton, M.; Bak, P. Criticality and scaling in evolutionary ecology. Trends Ecol Evol 14, 1999, 156–160.
3. Alonso, D.; Solé, R.V. Complexity and scaling in spatially extended ecosystems: On the role of instability. In: Complexity in Ecological Systems: On the Nature of Nature; Drake, J., Ed.; Columbia University Press; New York, to appear.
4. Solé, R.; Goodwin, B. Signs of Life. Basic Books: New York, 2000.
5. Bak, P.; Sneppen, K. Punctuated equilibrium and criticality in a simple model of evolution. Phys Rev Lett 71, 1993, 4083–4086.
6. Rhodes, B.; Anderson, R.M. Power laws governing epidemics in isolated populations. Nature 381, 1996, 600–602.
7. Rhodes, B.; Jensen, H.J.; Anderson, R.M. On the critical behavior of simple epidemics. Proc Roy Soc Lond B 264, 1997, 1639–1646.
8. Halley, J.M. Ecology, evolution and 1/*f* noise. Trends Ecol Evol 11, 1996, 33–37.
9. Sornette, D. Critical Phenomena in Natural Sciences. Springer-Verlag: Heidelberg, 2000.

10. Stanley, H.E. Introduction to phase transitions and critical phenomena. Oxford University Press: New York, 1987.
11. Bak, P.; Tang, C.; Wiesenfeld, K. Self-organized criticality: and explanation for 1/*f* noise. Phys Rev Lett 59, 1987, 381–384.
12. Jensen, H.J. Self-organized criticality. Cambridge University Press: Cambridge, 1998.
13. Solé, R.V.; Manrubia, S.C.; Benton, M.; Bak, P. Self-similarity of extinction statistics in the fossil record. Nature 388, 1997, 764–767.
14. Dickman, R.; Muñoz, M.A.; Vespignani, A.; Zapperi, S. Paths to self-organized criticality. Braz J Phys 30, 2000, 27–38.
15. Sornette, D.; Johansen, A.; Dornic, I. Mapping self-organized criticality onto criticality. J Phys I France 5, 1995, 325–335.
16. Vespignani, A.; Zapperi, S. Order parameter and scaling fields in self-organized criticality. Phys Rev Lett 78, 1998, 4793–4796.
17. Lipowski, A.; Lipowska, D. Nonequilibrium phase transition in a lattice prey-predator system. Phys A 276, 2000, 456–464.
18. Holling, C.S.; Gunderson, L.H. Resilience and adaptive cycles. In: Panarchy: Understanding Transformations in Human and Natural Systems; Gunderson, L.H.; Holling, C.S., Eds; Island Press: Washington, DC, 2002; pp 25–62.
19. Durrett, R.; Levin, S. Lessons on pattern formation from planet WATOR. J Theor Biol 205, 2000, 201–214.
20. Pascual, M.; Levin, S. From individuals to population densities: Searching for the intermediate scale of nontrivial determinism. Ecology 80, 1999, 2225–2236.
21. Pascual, M.; Roy, M.; Guichard, F.; Flierl, G. Cluster size distributions: signatures of self-organization in spatial ecologies. Phil Trans Roy Soc 357, 2002, 657–666.
22. Harris, T.E. Contact interactions on a lattice. Ann Prob 2, 1974, 969–988.
23. Durrett, R. Lecture Notes on Particle Systems and Percolation; Wadsworth Publishing Co.: Belmont, CA, 1988.
24. Pascual, M.; Mazzega, P.; Levin, S.A. Oscillatory dynamics and spatial scale: The role of noise and unresolved pattern. Ecology 82, 2001, 2357–2369.
25. Pascual, M.; Roy, M.; Franc, A. Simple temporal models for ecological systems with complex spatial patterns. Ecol Lett 5, 2002, 412–419.
26. Stauffer, D.; Aharony, A. Introduction to Percolation Theory. Taylor & Francis: London, 1994.
27. Pruessner, G.; Jensen, H.J. Broken scaling in the forest-fire model. Phys Rev E 65, 2002, 0567071–0567078.
28. Sander, L.M.; Warren, C.P.; Sokolov, I.M.; Simon, C.; Koopman, J. Percolation on disordered networks as a model for epidemics (preprint).
29. Minnhagen, P. The two-dimensional coulomb gas, vortex unbinding, and superfluid-superconducting films. Rev Mod Phys 59, 1987, 1001–1066.
30. Bramwell, S.T.; Christensen, K.; Fortin, J.Y.; Holdsworth, P.C.W.; Jensen, H.J.; Lise, S.; López, J.M.; Nicodemi, M.; Pinton, J.F.; Sellitto, M. Reply to comments on "Universal fluctuations in correlated systems." Phys Rev Lett 87, 2001, 188902–188901.
31. Cambier, J.L.; Nauenberg, M. Distribution of fractal clusters and scaling in the Ising model. Phys Rev B 34, 1986, 8071–8079.
32. Guichard, F.; Halpin, P.; Allison, G.; Lubchenco, J.; Menge, B. Mussel disturbance dynamics: signatures of oceanographic forcing from local interactions. Am Nat 2003, to appear.
33. Grassberger, P. On a self-organized critical forest-fire model. J Phys A 26, 1993, 2081–2089.
34. Clar, S.; Drossel, B.; Schenk, K.; Schwabl, F. Self-organized criticality in forest-fire models. Phys A 266, 1999, 153–159.
35. Janssen, M.A.; Andries, J.M.; Smith, M.S.; Walker, B.H. Implications of spatial heterogeneity of grazing pressure on the resilience of rangelands. In: Complexity and Ecosystem Management: The Theory and Practice of Multi-Agent Systems; Janssen, M.A., Ed.; Edward Elgar Publishers: Cheltenham, UK/Northampton, MA, 2002; pp 103–123.